# Investigation on Neutron Flux Effect onto Irradiated Fuel Burn-up Stored in the Reactor TRIGA PUSPATI

**M.A.A. Husain[1, 6*], S. Hashim[1, 2], D. Bradley[3, 4], M.H. Rabir[5], N. Zakaria[5] and M.R.M. Zin[5]**

[1]*Department of Physics, Faculty of Science, Universiti Teknologi Malaysia, 81310 UTM Skudai, Johor, Malaysia*
[2]*Centre for Sustainable Nanomaterials (CSNano), Ibnu Sina Institute for Scientific and Industrial Research (ISI-SIR), Universiti Teknologi Malaysia, 81310 UTM Skudai, Johor, Malaysia*
[3]*Department of Physics, Faculty of Engineering and Physical Sciences, University of Surrey, Guildford, United Kingdom*
[4]*Institute for Healthcare Development, Sunway University, 46150 PJ, Malaysia*
[5]*Malaysia Nuclear Agency, Bangi 43000 Kajang, Selangor, Malaysia*
[6]*Atomic Energy Licensing Board, 43800 Dengkil, Selangor, Malaysia*

## ARTICLE INFO

## ABSTRACT

An investigation on the out-core neutron flux in the Reactor TRIGA PUSPATI is carried out in this work to determine whether the thermal and/or fast neutron from the core would cause burn-up of the irradiated fuel stored in the same vicinity of the reactor core. The storage rack is positioned at 1 m from the central thimble. MCNPX code is used to calculate the fast and thermal neutron flux at 750 kW reactor power using 10 cm × 10 cm × 10 cm mesh while MATLAB model on 20 cm × 20 cm mesh model is used to plot the axial and radial distribution of the neutron flux density. The results show that the thermal neutrons occurred at energy lower than $1 \times 10^{-6}$ MeV and traveled to a maximum distance of 78 cm. The greatest flux for thermal and fast neutrons is $1 \times 10^{13}$ n.cm$^2$.s$^{-1}$ and $5 \times 10^{13}$ n.cm$^2$.s$^{-1}$ respectively. The fission-rate of the fuel in the core is determined to be $3.18 \times 10^{14}$ particle/s compared to $1.51 \times 10^7$ particle/s of the irradiated fuel in the storage rack. The burn-up of the fuel in the storage rack is in the order of micrograms and therefore is negligible. It is concluded that neutron flux from the core would not impart burn up effect onto the irradiated fuel stored at the storage rack in the reactor pool.

## INTRODUCTION

The PUSPATI TRIGA Mark II reactor (typically referred to by the acronym RTP, Reactor TRIGA PUSPATI) at the Malaysian Nuclear Agency, Malaysia, is the one and only research reactor in Malaysia. TRIGA stands for Training Research Isotopes, General Atomic while PUSPATI stands for Pusat Penyelidikan Tenaga Atom Tun Dr. Ismail (the Tun Dr Ismail Center for Atomic Energy Research). The reactor achieved its first criticality on June 28, 1982 and since then, it is operating for an average 500 hours per year.

The RTP is loaded with 3 types of standard TRIGA UZrH fuels of differing uranium composition: 8.5 wt %, 12 wt % and 20 wt %. The fuel is clad with stainless steel. In terms of the design, the RTP is a custom model that accommodates an out-core storage rack that has functions as a temporary storage for irradiated fuel, control rods and graphite rod. The rack is located 1 m from the central thimble of the core.

Nuclear fuel utilization in a reactor is referred to the burn-up. The burning of the nuclear fuel is a neutronic process, depending on neutron-induced fission. In the RTP, an americium-beryllium (Am-Be) source is used as the neutron source in order to initiate the fission process. The fission process emits more neutrons from the fuel in

the form of fast neutron, epithermal/intermediate neutrons and thermal neutrons. Each neutron also has difference energy to travel from core to paranomic direction in the reactor pool through the moderator[1]. These neutrons are subjected to migration, diffusion and slowing-down process. Neutrons are moderated and then diffused in thermal energy region and finally absorbed in surrounding media. It is assumed that there are leaked neutrons i.e. nuetrons that escape from the vicinity of the fissionable material in the reactor core; that travel relatively far distance from the core, hence there is a possibility of fast neutron being thermalized and absorbed by irradiated fuels stored at the storage rack and induced fission.

The objective of this work is to investigate the effect of neutron flux from the core onto the irradiated fuel stored at the storage rack in the reactor pool. In other words, this work investigates whether the thermal and/or fast neutron flux would cause burn-up of the irradiated fuel stored at the storage rack in the same vicinity of the reactor core. The neutron flux ($\phi$) is a measure of the intensity of neutron radiation, determined by the flowrate of neutrons. The neutron flux value is calculated as the neutron density ($n$) multiplied by neutron velocity ($v$), where $n$ is the number of neutrons per cubic centimeter (expressed as neutrons/cm$^3$) and $v$ is the distance the neutrons travel in 1 second (expressed in cm/s). The unit for neutron flux is n.cm$^2$.s$^{-1}$.

From the neutron flux, the reaction rate (RR) which is the number of interactions taking place in that cubic centimeter in one second can be calculated, given by:

$$RR = \phi \; x \; \Sigma = \phi \; x \; N \; x \; \sigma \tag{1}$$

where $\phi$ is neutron flux, $N$ is the atomic number density and $\sigma$ is microscopic cross section.

The atomic number density is given by:

$$N_i = \frac{Av \; x \; \rho \; x \; \omega_i}{M_i} \tag{2}$$

where $Av$ is Avogadro's number, $\rho$ is material density, $\omega_i$ is weight fraction of material and $M_i$ is molar mass of material.

The Fission Rate, is calculated from the reaction rate as follows:

$$Fission \; rate = RR \; x \; V \tag{3}$$

where $V$ is volume.

A method to solve the neutron transport equation is by using Monte Carlo which is a stochastic statistical simulation method. The Monte Carlo N-Particle (MCNP) code is capable to provide correct representation of detailed geometry, transport effects and continuous energy cross sections [2]. It is a favored choice because of its general modeling capability, correct representation of detailed geometry, transport effects and continuous energy cross-sections. There are numerous codes that use the Monte Carlo method, the widest spread being used is Monte Carlo N-Particle Extended (MCNPX) utilized to calculate the interrogating neutron flux and predict acquired spectra accounting for the interrogation geometry and detector effect [3]. Table 1, adapted from the study conducted by Alnour *et al.* [4], summarizes the neutron flux profile in the RTP calculated using MCNPX.

**Table 1**. Recorded average thermal neutron flux and epithermal neutron flux in the RTP calculated using MCNPX.

| Study | Year | Thermal neutron flux (x $10^{12}$ n cm$^{-2}$ s$^{-1}$) | Epithermal neutron flux (x $10^{11}$ n cm$^{-2}$ s$^{-1}$) |
|---|---|---|---|
| Alnour [4] | 2013 | $2.33 \pm 0.08$ | $1.23 \pm 0.02$ |
| Liew [5] | 2010 | $2.26 \pm 0.10$ | $1.11 \pm 0.11$ |

The burn-up refers to the utilization of nuclear fuel in the reactor and a burn-up rate represents the fuel mass fissioned per unit time determined as follows:

$$Burnup \; Rate = Fission \; Rate \; x \; \frac{M_{235}}{Av} \tag{4}$$

where $M_{235}$ is 235 g/mol and $Av$ is Avogadro's number

The burn-up parameters can be obtained from measurement of the neutron flux produced by the burn-up-dependent neutron source in a spent fuel bundle [6]. Several studies on burn-up determination of TRIGA fuel in the core were conducted by many researchers [7-8] however, there is no discussion on burn-up for out-core fuel.

## METHODOLOGY

In this work, the computational model was created using MCNPX version 2.7 with evaluated nuclear data file for thermal neutron scattering law data (ENDF7) cross-section data library. Core 15 configuration is used in the calculation (Fig.1). Tallies F1, F4 and F8 are the most important output data, which refers to counts of particles passing a given surface (F1), mapping of thermal neutron travel through the moderator in the reactor pool (F4) and radiation pulses (F8). The MCNP model developed in this study is a full 3D model as shown

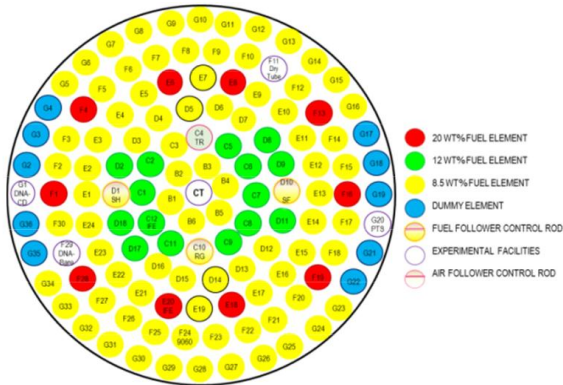in Fig. 2. The mesh size adopted for this model is 10 cm × 10 cm × 10 cm.



**Fig. 1**. Cross-sectional view of Core Configuration No. 15.
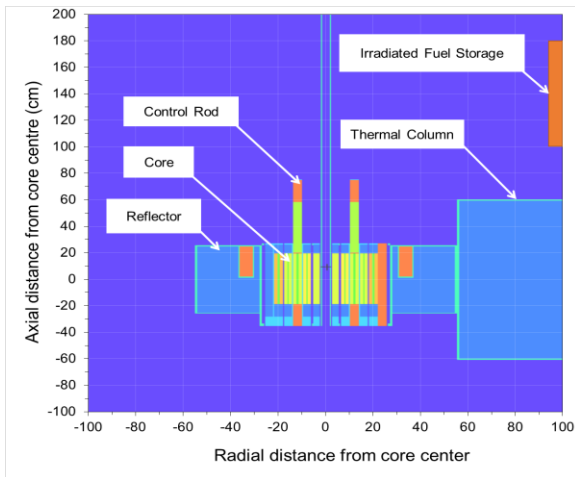


**Fig. 2**. Axial view of the MCNPX model for the RTP.

Two irradiated fuels are selected for this works representing 20 wt% fuel type and 8.5 wt% fuel type. The respective fission rate for the fuel is $7.07 \times 10^7$ reaction per second and $3.93 \times 10^6$ reaction per second. The geometrical model constructed for the irradiated fuel sliced the fuel cladding into several layers to allow for flux tally calculation as shown in Fig. 3.
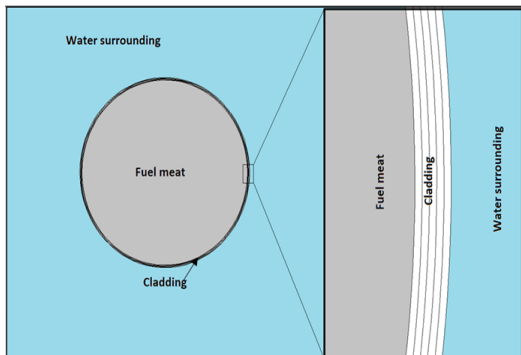


**Fig. 3**. MCNP Geometrical Model of the Irradiated Fuel.

## RESULTS AND DISCUSSION

The path of neutron distribution, representing the distance a neutron travels between interactions, depends on both the type of material and the energy of the neutron. After each collision, the energy is decreased and the neutron path length is affected accordingly. The global simulation output illustrated in Fig. 4 shows the neutron track in surrounding water of the irradiated fuel stored at the storage rack 1 m from the central thimble.
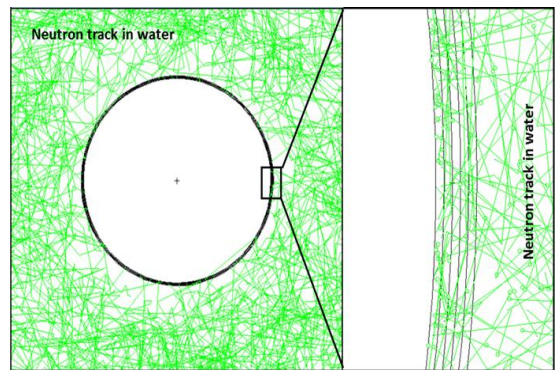


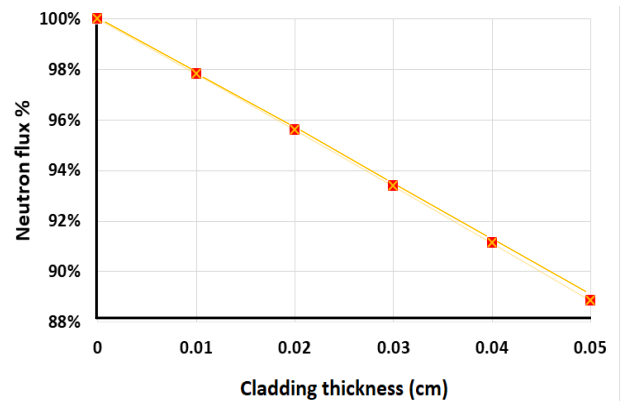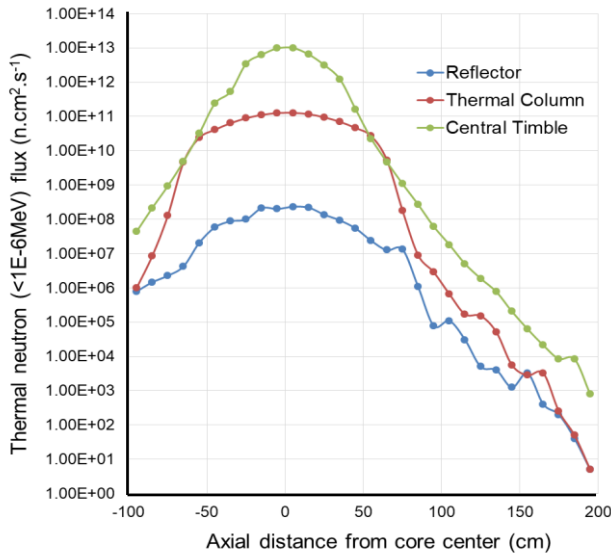**Fig. 4**. Neutron track in water surrounding the fuel at the storage rack.



**Fig. 5**. Percentages of neutron flux across the cladding thickness.

Upon collision, the neutron flux reduces across the cladding material. Fig. 5 shows that the flux reduces in a linear fashion for the 0.05 cm cladding thickness resulting in a neutron flux reduction by 14.5 %. The result is consistent with the observation that has been made according to the behaviors of the thermal neutron flux, which is the dominant neutron flux in the reactor (neutrons are well thermalized with about 95 % of thermal over epithermal neutrons) [9]. The axial thermal neutron flux at full core power of 750 kW is presented in Fig. 6. The profile of the thermal neutron flux distributions displays the typical 'bell-shape' for the axial distance from core center between -100 cm to +100 cm, while a rapid decline of the flux occurs

from the axial distance of +100 cm up to +200 cm, which was consistently with normalized neutron flux shape form experiment that has been conducted previously [10]. The flux shape relates to the density or relative strength of the flux as it moves around the reactor core.
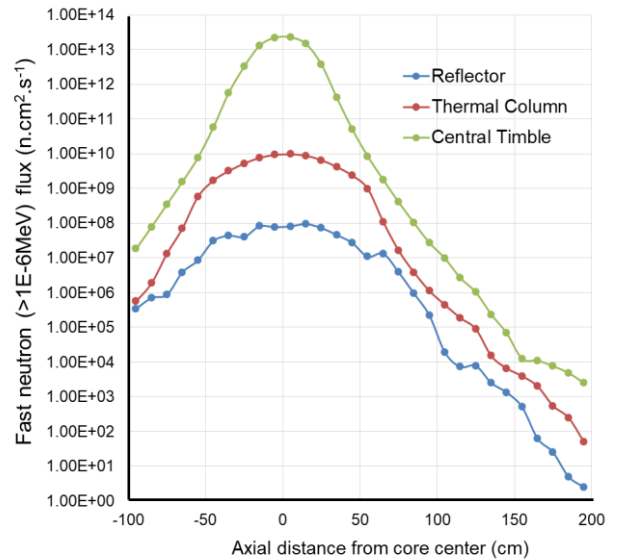
trend from +100 cm up to +200 cm. The 'bell-shape' becomes less apparent for the fast neutron flux at the reflector and the thermal column as a result of attenuation due to scattering and collisions. The maximum fast neutron flux is observed to occur at the central thimble, at $5 \times 10^{13}$ n.cm$^2$.s$^{-1}$ due to its central position in the core.



**Fig. 6**. Axial thermal neutron (<1E-6MeV) flux (n.cm$^2$.s$^{-1}$) profile at full core power of 750 kW.

The reactivity normally is larger at the center of the core [11]. As indicated in Fig. 6, the thermal neutron flux is greatest at the central thimble position at $1 \times 10^{13}$ n.cm$^2$.s$^{-1}$ while the maximum neutron fluxes at the thermal column and at the reflector are greatly reduced to $1 \times 10^{11}$ n.cm$^2$.s$^{-1}$ and $4 \times 10^8$ n.cm$^2$.s$^{-1}$ respectively as a result of elastic and inelastic neutron-nucleus scattering collisions. The thermal and fast neutron flux were reported to be concentrated at the central thimble [12], while there was a significant reduction of the flux particularly at the position of the DNA-Cd monitor due to the thermal neutrons being absorbed by the cadmium.

The fast neutron (neutrons energy higher than $1 \times 10^{-6}$ MeV) travel profile is analyzed in this work. The distance that a fast neutron will travel, between its introduction into the slowing down medium (moderator) and thermalization, is dependent on the number of collisions and the distance between collisions. Though the actual path of the neutron slowing down is tortuous because of collisions, the average straight-line distance can be determined. This distance is called the fast diffusion length or slowing-down length [13]. A similar pattern to that of the thermal neutrons is obtained for the fast neutrons as shown in Fig. 7, with a 'bell-shape' flux distribution occurring between -100 cm and +100 cm from the core. The fast neutron flux then shows a declining



**Fig. 7**. Axial fast neutron (>1E-6MeV) flux (n.cm$^2$.s$^{-1}$) profile at full core power of 750 kW.

When the neutron flux density is plotted using MATLAB on the 20 cm × 20 cm grid, the distance travelled by the thermal neutrons can be determined. Fig. 8 illustrates the contour of the thermal neutron flux axial distribution. The red/orange region represents thermal neutrons with fluxes between $1 \times 10^9$ n.cm$^2$.s$^{-1}$ and $1 \times 10^{12}$ n.cm$^2$.s$^{-1}$ while the green region plots the thermal neutron with fluxes between $1 \times 10^5$ and $1 \times 10^9$ n.cm$^2$.s$^{-1}$.
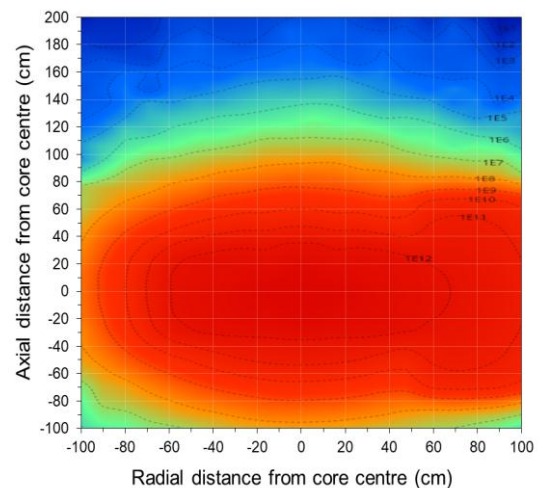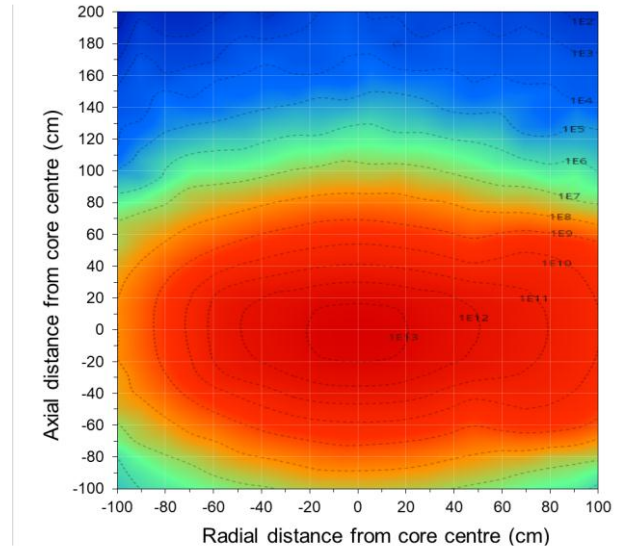


**Fig. 8**. Axial distribution of thermal neutron contour flux at full core power of 750 kW.

The greatest flux of thermal neutron is determined to be $1 \times 10^{13}$ n.cm$^2$.s$^{-1}$. The farthest distance travelled by thermal neutron is 78 cm, observed from flux at $1 \times 10^8$ n.cm$^2$.s$^{-1}$. When Fig. 8 is interpreted with the corresponding radial distribution in Fig. 9, the result indicated that the epithermal region of the neutron flux started is between 78 cm and 158 cm from the core. The thermalization process in this region occurs rapidly, attributed to water being an effective moderator, with hydrogen being of similar size to the neutron. These observations show that the thermal neutron is being thermalized at 78 cm.
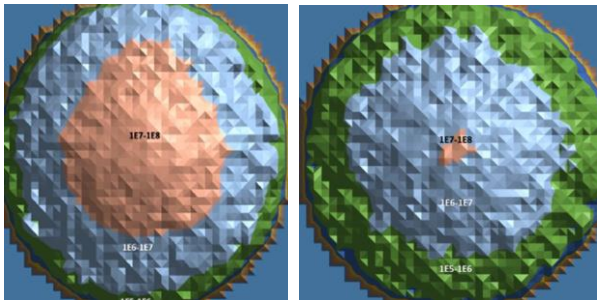


**Fig. 9**. Radial distribution of thermal neutron flux at full core power of 750 kW at 1 meter from irradiated fuel storage.

**Fig. 10**. Radial distribution of fast neutron flux at full core power of 750 kW at 1 meter from irradiate fuel storage.

The 3D radial distribution view for the fast neutron fluxes is shown in Fig. 10 and the axial flux distribution contour for fast neutron is depicted in Fig. 11. The greatest fast neutron flux is determined to be $5 \times 10^{13}$ n.cm$^2$.s$^{-1}$. The red/orange region in Fig. 10 shows the fast neutrons with fluxes between $1 \times 10^7$ n.cm$^2$.s$^{-1}$ and $1 \times 10^{13}$ n.cm$^2$.s$^{-1}$ while the green region maps fluxes between $1 \times 10^2$ and $1 \times 10^9$ n.cm$^2$.s$^{-1}$. The fluxes in the red region are attributed to fission reaction, and as the neutron lose their kinetic energy, the fluxes reduce accordingly. In the blue region, the neutrons have lost their kinetic energy to a point where they are in thermal equilibrium with the surrounding gas molecules and are then considered to be "thermalized." Once "thermalized," these neutrons have a high likelihood of being captured by absorbing nuclei.



**Fig. 11**. Axial distribution of fast neutron flux contour at full core power of 750 kW.

While thermalization is mainly due to water moderation, to a certain extent it is also due to the graphite at the thermal column. Base on reported that the decay constant of neutron flux in graphite was 2341/s [14]. The thermalization by graphite occurred in 250 μsec to 750 μsec depending on the degree of graphite buckling.

As indicated in Table 2, the calculational result shows that the fission-rate of the fuel in the core is $3.18 \times 10^{14}$ particle/s compared to $1.51 \times 10^7$ particle/s of the irradiated fuel at the storage rack, indicating the fission-rate in the storage rack is negligible compared to the fission-rate at the core. This is consistent with the flux distribution contour discussed earlier. Assuming that an irradiated fuel is to be stored in the storage rack for the next 30 years, with continuous 24/7 exposure to a power level of 750 kW, the simulation confirms that the level of the associated burn-up would be negligible, as depicted in Table 3. Only less than 2 μg of U-235 will be burned throughout this span of storage period for the 8.5 wt% fuel type and less than 30 μg for the 20 wt% fuel type. Therefore, the calculation shows that to a practical extent, the neutron does not induce burn-up in the irradiated fuel at the storage rack.

**Table 2.** Irradiation of a single fuel in the core and in the fuel rack above the core.

| Fuel Location | At 750 kW Core Power Level | | | At 1kW Core Power Level | | |
|---|---|---|---|---|---|---|
| | Fission Rate (#/s) | Energy Release (Watt) | U-235 burned (in g) from 38g initial mass after 1 day | Fission-Rate (#/s) | Energy Release (Watt) | U-235 burned (in g) from 38g initial mass after 1 day |
| Fuel in-core | $3.18 \times 10^{14}$ | $1.02 \times 10^4$ | $1.26 \times 10^{-2}$ | $4.24 \times 10^{11}$ | $1.36 \times 10$ | $1.68 \times 10^{-5}$ |
| Irradiated fuel in storage rack (out-core) | $1.51 \times 10^7$ | $4.84 \times 10^{-4}$ | $6.01 \times 10^{-10}$ | $2.02 \times 10^4$ | $6.46 \times 10^{-7}$ | $8.01 \times 10^{-13}$ |

**Table 3**. Burn-up rate of one fuel element located at storage rack.

| RTP operation period (year) at full power continuous 365 days per year and 24 hours per day | U-235 burned (g) from 8.5 wt% fuel type initial mass | Burn-up [%] of 8.5 wt% fuel type | U-235 burned (g) from 20 wt% fuel type initial mass | Burn-up [%] of 20 wt% fuel type |
|---|---|---|---|---|
| 1 | $5.12 \times 10^{-08}$ | $0.00 \times 10^{-06}$ | $9.22 \times 10^{-07}$ | $2.00 \times 10^{-06}$ |
| 2 | $1.02 \times 10^{-07}$ | $0.00 \times 10^{-06}$ | $1.84 \times 10^{-06}$ | $5.00 \times 10^{-06}$ |
| 3 | $1.54 \times 10^{-07}$ | $0.00 \times 10^{-06}$ | $2.77 \times 10^{-06}$ | $7.00 \times 10^{-06}$ |
| 4 | $2.05 \times 10^{-07}$ | $1.00 \times 10^{-06}$ | $3.69 \times 10^{-06}$ | $1.00 \times 10^{-05}$ |
| 5 | $2.56 \times 10^{-07}$ | $1.00 \times 10^{-06}$ | $4.61 \times 10^{-06}$ | $1.20 \times 10^{-05}$ |
| 6 | $3.07 \times 10^{-07}$ | $1.00 \times 10^{-06}$ | $5.53 \times 10^{-06}$ | $1.50 \times 10^{-05}$ |
| 7 | $3.58 \times 10^{-07}$ | $1.00 \times 10^{-06}$ | $6.45 \times 10^{-06}$ | $1.70 \times 10^{-05}$ |
| 8 | $4.10 \times 10^{-07}$ | $1.00 \times 10^{-06}$ | $7.38 \times 10^{-06}$ | $1.90 \times 10^{-05}$ |
| 9 | $4.61 \times 10^{-07}$ | $1.00 \times 10^{-06}$ | $8.30 \times 10^{-06}$ | $2.20 \times 10^{-05}$ |
| 10 | $5.12 \times 10^{-07}$ | $1.00 \times 10^{-06}$ | $9.22 \times 10^{-06}$ | $2.40 \times 10^{-05}$ |
| 20 | $1.02 \times 10^{-06}$ | $3.00 \times 10^{-06}$ | $1.84 \times 10^{-05}$ | $4.90 \times 10^{-05}$ |
| 30 | $1.54 \times 10^{-06}$ | $4.00 \times 10^{-06}$ | $2.77 \times 10^{-05}$ | $7.30 \times 10^{-05}$ |

## CONCLUSION

MCNPX code was used to simulate fast and thermal neutron flux for reactor operating at 750 kW, using a 10 cm × 10 cm × 10 cm mesh model. For fast neutron, the energy is higher than $1 \times 10^{-6}$ MeV and travels more than 158 cm indicating that the fast neutron can travel far distance reaching the area of the fuel rack.

The reaction time for the fast neutron is too short to result in burn-up due to short interaction time. Thermal neutron in-core travels maximum distance of 78 cm due to thermalization by moderator, thus it is confirmed that the thermal neutron from the core does not reach to the storage rack.

The axial distribution for thermal neutrons occurred at energy lower than $1 \times 10^{-6}$ MeV. Above this energy, the neutrons are regarded as epithermal and/or fast neutrons. The fission reaction of the irradiated fuel in the fuel rack is 7 order of magnitude lower than the fission rate at the core, indicating very small to negligible fission reaction of these fuels.

The results presented in this works conclude that the neutron flux from the core would not impart burn-up effect onto irradiated fuel stored at the storage rack in the pool.

## REFERENCES

1. G. Fioni, M. Cribier, F. Marie *et al.*, Nucl. Phys. A **693** (2001) 546.

2. B.El. Bakkari, T.El. Bardouni, B. Nacir *et al.*, Ann. Nucl. Energy **51** (2013) 112.

3. Anonymous, *MCNPX™ User's Manual, Version 2.60*, D.B. Pelowitz (Ed.), Los Alamos National Laboratory 2008, LA-CP-07-1473 (2008).

4. I.A. Alnour, H. Wagiran, N. Ibrahim *et al.*, J. Radioanal. Nucl. Chem. **296** (2013) 1231.

5. H.F. Liew, The Absolute Method of Neutron Activation Analysis Using TRIGA Neutron Reactor, MSc. Dissertation, Universiti Teknologi Malaysia (2010).

6. M. Ueda, S. Kikuchi, T. Kikuchi *et al.*, J. Nucl. Sci. Technol. **30** (1993) 48.

7. M.H. Rabir, M.D. Usang, N.S. Hamzah *et al.*, Sains Nuklear Malaysia **25** (2013) 46.

8. L. Snoj, A. Trkov, R.I. Jac *et al.*, Appl. Radiat. Isot. **69** (2011) 136.

9. I.A. Alnour, N. Ibrahim and H.F. Liew, Phys. Sci. **6** (2011) 4169.

10. Y. Yamane, A. Uritani, T. Misawa *et al.*, Nucl. Instrum. Methods Phys. Res., Sect. A **432** (1999) 403.

11. T. Matsumoto, J. Nucl. Sci. Technol. **35** (1998) 662.

12. S. Sangkaew, T. Angwongtrakool and B. Srimok, Physics **860** (2017) 012033.

13. A.W. Ajlouni, A. Al-Okour and A. Ajlouni, Math. Analysis **6** (2012) 437.

14. J. Mitsui and K. Sugiyama, J. Nucl. Sci. Technol. **10** (1973) 19.